






Acidic wood extractives accelerate the curing process of emulsion polymer isocyanate adhesives

Merve Özparpucu¹  | Antoni Sánchez-Ferrer¹  | Mathias Schuh¹ |
 Bianca Wilhelm¹ | Riddhiman Sarkar^{2,3}  | Bernd Reif^{2,3}  |
 Elisabeth Windeisen-Holzhauser¹ | Klaus Richter¹ 

¹School of Life Sciences Weihenstephan, Chair of Wood Science, Technical University of Munich, Munich, Germany

²Deutsches Forschungszentrum für Gesundheit und Umwelt, Helmholtz-Zentrum München (HMGU), Neuherberg, Germany

³Department of Chemistry, Technical University of Munich, Bayerisches NMR Zentrum (BNMRZ), Garching, Germany

Correspondence

Merve Özparpucu and Antoni Sánchez-Ferrer, School of Life Sciences Weihenstephan, Chair of Wood Science, Technical University of Munich, Winzererstr. 45, Munich, 80797, Germany. Email: oezparpucu@hfm.tum.de and sanchez@hfm.tum.de

Funding information

Bundesministerium für Wirtschaft und Energie, Grant/Award Number: IGF 19314 N

Abstract

Emulsion polymer isocyanate (EPI) adhesive is one of the most widely used structural adhesives in the woodworking industry. However, there has been a lack of knowledge on how the EPI-adhesive interacts with the chemical constituents of wood, in particular, with the wood extractives that are known to influence the bonding quality. In this study, the interactions of the EPI-adhesive with the water extracts and selected extractives from European wood species were systematically investigated using different analytical techniques. While the alterations in the curing properties of the pure EPI-adhesive and EPI-adhesive-extract mixtures were revealed by in situ rheology and Fourier-transform infrared spectroscopy, evolved gas analysis, and pyrolysis-gas chromatography/mass spectrometry, the solid-state ¹³C nuclear magnetic resonance were performed for analyzing the final chemical composition of the cured adhesive. Moreover, the influence of the extraction on the mechanical bonding performance was tested by tensile-shear tests. The study revealed significant interactions between the EPI-adhesive and tannin-rich, acidic wood extracts. The acidic chestnut and oak extracts catalyzed the curing reactions and led to a huge increase in the adhesive viscosity. These interactions might affect the bonding quality, for example, adhesive penetration depth and formation of bonding strength, therefore, careful attention is required when bonding acidic wood surfaces.

KEYWORDS

adhesive, ATR-FTIR spectroscopy, extracts, EPI, NMR, rheology, wood bonding

1 | INTRODUCTION

Wood is a versatile, natural hierarchically structured material that its' cell walls can be considered as a fiber composite composed of cellulosic microfibrils embedded

in the hemicellulose-lignin matrix. In addition to the aforementioned major wood polymers, some minor wood components-so called extractives- can be present which are often specific for wood species and responsible for some properties such as color and durability. Driven by

This is an open access article under the terms of the Creative Commons Attribution License, which permits use, distribution and reproduction in any medium, provided the original work is properly cited.

© 2022 The Authors. *Journal of Applied Polymer Science* published by Wiley Periodicals LLC.

the necessity for renewable and low emission products, there has been an increasing demand for wood-based materials.^{1,2} Developments in adhesive wood bonding allow for the production of efficient wood assemblies. However, there have been challenges in the wood bonding process due to the inherently complex chemical and structural properties of the wood species. Although wood extractives are the minor compounds of the chemical wood constituents, they might have a significant influence on the wood bonding quality as they can migrate to the wood surface during the finishing and bonding process. Their presence on the wood surface might create a physical barrier for the penetration of the adhesives.³ Such a barrier can be responsible for the lower mechanical interlocking capability of the adhesive in the subsurface cell layer, resulting evidently in lower mechanical strength of the bonded wood assemblies. It has been shown that extractives were responsible for a reduced wettability of southern pine bark revealed by diethyl ether extraction,⁴ whereas, in another study, the wettability of southern yellow pine wood decreased after extraction by an ethanol-toluene mixture.⁵ The extraction-wettability relation is still under debate due to the complex nature of the wood surface chemistry (i.e., extractives nature, extraction amount, some other additional surface inactivation mechanisms such as micropore closure, molecular orientation, etc.).

Next to these physical effects mentioned above, extractives can interfere also chemically with the reactive adhesive during the curing process. Such interactions are known to be more common for hardwood species. In one of the studies, it was shown that the acidic oak extractives resulted in a significant loss of the bond strength when using phenolic adhesives.⁶ Similarly, prolonged curing times for the phenolic adhesives were reported when gluing oak and Kapur.⁷ On the other hand, an acceleration of the curing process was observed for phenol-formaldehyde resin in the presence of Merbau wood extractives with a high presence of flavonoids.⁸ Recently, it has been reported that chestnut extract—with gallic acid as the major component of the chestnut extract—resulted in a delay in the curing reactions of melamine-urea-formaldehyde (MUF) adhesive.⁹ Drawing a general conclusion regarding the effects of the extractives on the curing process of wood adhesive is unfeasible. Therefore, more systematic studies and specific analyses are required for each wood adhesive type and wood species.

Emulsion polymer isocyanate (EPI) adhesives are two-component systems consisting of a water-based emulsion—a latex-containing hydroxyl groups polymer, for example, poly(vinyl alcohol) (PVA), ethylene-vinyl acetate (EVA)—and an isocyanate as a hardener or crosslinker—polymeric methylene diphenyl diisocyanate

(pMDI)—which was first developed in Japan in the early 1970s.¹⁰ By the beginning of the 1990s, there has been an increasing demand for EPI adhesives also in Europe and the United States as it brings some important advantages in comparison to the common water-based polycondensation adhesives, for example, fast setting and curing even at ambient temperatures, good creep and moisture resistance, and light-color appearance of the glue line.^{10–13} More importantly, EPI adhesives are formaldehyde-free systems.¹⁴ They are mostly applied for nonstructural applications in the woodworking industries (parquet, edge-glued solid wood panels), but specific systems got also approval for load-bearing glued laminated timber.¹⁵ As two-component adhesive systems, they are also promoted for gluing difficult wood species like hardwoods. However, to the best of our knowledge, there has been a very limited number of studies so far investigating the interactions of the wood extractives with EPI adhesives.¹⁵

Hence, in this study, the influence of wood extracts and selected extractives on the EPI-adhesive curing process was investigated systematically using a Fourier-transform infrared (FTIR) spectrophotometer with an attenuated total reflection (ATR) mode and coupled to a rheometer,¹⁶ which enables in situ information both on the chemical (curing reaction) and physical (hardening) evolution, respectively, of the EPI-adhesive and its' mixtures with different wood extractives during the curing process. As the EPI-adhesive is also a water-based adhesive system, the influence of the water-soluble extractives was investigated. Complementary to the FTIR analysis, the chemical composition of the cured adhesives with or without the presence of extractives was investigated in detail using solid-state ¹³C nuclear magnetic resonance (ssNMR), whereas evolved gas analysis (EGA) and pyrolysis-gas chromatography-mass spectrometry (py-GC/MS) were performed to investigate the thermal decomposition profile and the volatile compounds that arise from the adhesive. Finally, tensile-shear strength experiments on EPI-glued wood bond lines were performed and correlated with the analyzed chemical and rheological properties.

2 | MATERIALS AND METHODS

2.1 | Wood species and extraction analysis

Seven different European wood species—spruce (*Picea abies*), pine (*Pinus sylvestris*), Douglas fir (*Pseudotsuga menziesii*), larch (*Larix decidua* Mill), beech (*Fagus sylvatica* L.), oak (*Quercus* spp.) and chestnut (*Castanea sativa*)—were chosen for the extraction in water at room

temperature for 48 h (Özparpucu et al. 2020). The chemical analysis of extracts was performed by FTIR spectroscopy (iS 50 FTIR Nicolet, Thermo Scientific Fischer) and 1% extracts in KBr pellets were prepared. The spectra were recorded by accumulating 32 scans at 4 cm^{-1} resolution in the mid-infrared region ($400\text{--}4000\text{ cm}^{-1}$). The baseline-corrected spectra were exported to Unscrambler Software (Camo Analytics) for further statistical analysis.

2.2 | In situ rheology-FTIR measurements

The rheological evolution during the curing process was monitored with a Haake Mars 40 Rheometer (Thermo Scientific Fischer) in oscillation mode using a plate-plate geometry with an upper plate diameter of 25 mm and a measuring gap of 0.5 mm during 180 min at 20°C . The oscillation parameters were set to a strain value of 0.1% and at a frequency of 1 Hz ($\omega = 6.28\text{ rad/s}$). The excess of the sample outside the plates was trimmed and the edge was sealed with silicone oil to prevent the reaction of the adhesive with the external humidity.

Parallel to the rheological measurement, the FTIR absorbance of the sample was measured from 400 to 4000 cm^{-1} with a spectral resolution of 4 cm^{-1} , and one spectrum was recorded per minute. Baseline corrected and normalized spectra with respect to the absorption peak at 873 cm^{-1} (Figure S1) were further evaluated using Unscrambler Software (Camo Analytics).

For long-time rheological experiments, some selected samples were measured for 36 h with an Anton Paar (MCR 301) rheometer using a plate-plate geometry with an upper plate diameter of 25 mm and a measuring gap of 0.5 mm at 20°C , at 0.1% strain and 1 Hz frequency.

The sample preparation consists of mixing the water-based resin (Preferre 6183 from Dynea) with the hardener (Preferre 6683 from Dynea) at a ratio of 5:1 with a constant mixing time of 40 s before loading the sample on the rheometer plate. A reference sample was prepared by mixing both EPI-adhesive components. In order to mimic the real bonding conditions as accurately as possible,⁹ different extract amounts were mixed with the EPI adhesive formulation (Table 1). Therefore, an approximate amount of wood extracts was calculated for each wood specie bonding surface in the proportion of the total surface area, using the extraction results as published previously.⁹

2.3 | Evolved gas analysis

The EGA measurements were performed with a double shot pyrolyzer Py-2020iD (Frontier Laboratories)

TABLE 1 The sample codes, extract addition (%), and the number of measurements performed

Samples ^a	Extract addition (%) to EPI	Number of measurements (<i>n</i>)
EPI-Ref	—	6
EPI-Sp	0.067	3
EPI-Pi	0.558	5
EPI-Do	0.139	3
EPI-La	0.652	3
EPI-Be	0.170	3
EPI-Oa	0.179	5
EPI-Ch	0.916	5

Abbreviation: EPI, emulsion polymer isocyanate.

^aReference sample (Ref), spruce (Sp), pine (Pi), Douglas fir (Do), larch (La), beech (Be), oak (Oa), chestnut (Ch).

connected to a 5975C Series GC/MSD system (Agilent Technologies). Hundred micrograms of EPI-Ref and selected EPI/extractives mixtures were put into a stainless steel cup (Eco cup, Frontier Laboratories) to be inserted into the pyrolysis furnace. Two measurements were done on each sample ($n = 2$). The samples were heated continuously from 50 up to 750°C at a heating rate of $10^\circ\text{C}/\text{min}$, whereas the GC oven and the inlet were held isothermally at 300°C . The evolved gases were transferred via a deactivated stainless steel EGA column ($2.5\text{ m} \times 0.15\text{ mm}$) to the MS detector without any chromatographic separation. Noteworthy, the measurements were performed directly after the rheology measurements (i.e., after 180 min, at not the fully cured state of the adhesive).

2.4 | Pyrolysis-gas chromatography/mass spectrometry (Py-GC/MS)

Pyrolysis experiments were performed directly after the rheology measurements as well. Based on the differences in the thermal desorption isotherms between the samples taken by EGA, double shot analysis (DSA) was performed on the selected samples. DSA allowed determining the volatile components of the adhesive systems sequentially. In the first thermal desorption (TD) stage, the EPI adhesives were heated at 200°C for 0.2 min in the pyrolysis oven (Py-2020iD, Frontier Laboratories). The resulting volatile compounds were trapped at the beginning of the GC column ($30\text{ m} \times 0.25\text{ mm} \times 0.25\text{ }\mu\text{m}$, VF-17 ms, Agilent Technologies) and analyzed via GC/MS (5975C Series GC/MSD system, Agilent Technologies). After the TD stage, the residual sample was pyrolyzed at 310°C for 0.2 min. The emerging pyrolysis products were analyzed

with GC/MS as well. For both thermal desorption and pyrolysis steps, the GC oven was set to 50°C with a holding time of 1 min, then, heated to 300°C at a heating rate of 10°C/min. Finally, it was kept at 300°C for 4 min. The mass spectrometer was operated in EI mode (70 eV, scanning m/z 40–700 Da). The MS transfer line temperature was 250°C. The MS ion source temperature was fixed at 230°C and the MS quadrupole temperature at 150°C.

2.5 | Liquid and solid-state NMR

Liquid ^{13}C -NMR and DEPT experiments were carried out at room temperature on a Bruker Avance Spectrometer AVHD400 operating at 100 MHz (^{13}C), and using CDCl_3 or $\text{DMSO-}d_6$ as solvents and as the internal standards. Chemical shifts simulations were performed with MestReNova Software. The EPI-emulsion (PVA-PVAc) was dried and measured in $\text{DMSO-}d_6$ - ^{13}C NMR (100 MHz, $\text{DMSO-}d_6$): $\delta = 169.8$ (COO), 66.7 (CH—OAc), 64.4 (CH—OH), 46.3 ($\text{CH}_2\text{CH—OAc}$), 38.8 ($\text{CH}_2\text{CH—OH}$) 20.8 ($\text{CH}_3\text{C=O}$) ppm⁻, the EPI-hardener (pMDI) was directly measured in CDCl_3 - ^{13}C NMR (100 MHz, CDCl_3): $\delta = 138.5$ (i-Ar), 131.7 (p-Ar), 130.1 (o-ArH), 125.0 (m-ArH), 124.8 (N=C=O), 40.8 (CH_2) ppm⁻, and the chestnut extractive was measured in $\text{DMSO-}d_6$ - ^{13}C NMR (100 MHz, $\text{DMSO-}d_6$): $\delta = 167.7$ (COOH), 145.6 (m-Ar), 138.2 (p-Ar), 120.6 (i-Ar), 108.9 (o-ArH). 95–98 (O—CH—OH, sugars), 74–78 (CH—O, sugars), 69–74 (CH—OH, sugars, and inositol), 60–63 (CH_2 —OH, sugars) ppm.

All solid-state ^{13}C NMR experiments were carried out employing a B_0 field of 9.4 T (400 MHz for protons), a 3.2 mm H/C/N/D four-channel probe, and MAS frequency of 18 kHz. RF fields of $\omega_1(^{13}\text{C})/2\pi \sim 43$ kHz and $\omega_1(^1\text{H})/2\pi \sim 70$ kHz with a 70–100 ramped shape on the ^1H channel were used for Hartmann-Hahn cross-polarization, where the contact time for $^1\text{H} \rightarrow ^{13}\text{C}$ transfer was set to 2 ms. SPINAL64 decoupling with $\omega_1(^1\text{H})/2\pi \sim 100$ kHz was employed during acquisition with a recycle delay of 3 s.

2.6 | Tensile-shear tests

Chestnut wood boards sawn were stored for several months in a climate room at 20°C and 65% RH, resulting in a wood moisture content of $12\% \pm 1\%$. For the mechanical tests, wood boards were chosen based on the wood quality specifications of the DIN EN 302-1:2013 standard. The selected boards were processed into 16 panels with dimensions of $30 \times 15 \times 1$ cm³ (length, width, and thickness). To investigate the influence of extracts on the wood bonding strength, eight panels were

extracted using water as a solvent, and eight were kept as a reference without any treatment.

For the extraction, four panels were put into a water container filled with deionized water at 20°C with a volume wood/water ratio of 1:13 (Figure S2a). The water media was stirred continuously with a magnetic stirrer. After 50 h, the water solution in the container was exchanged with fresh deionized water and the extraction was stopped after an additional 30 h. After both 50 h and 80 h, 300 ml of each extractives solution was concentrated in a rotary evaporator, fully dried by freeze-drying the samples, and the percentage of solids (extracts) was calculated gravimetrically.

After the extraction process, the wood panels were dried at 30°C and reconditioned in a climate room (at 20°C and 65% RH) until constant mass for 24 h (weight difference <0.1%).

All panels were planed to a thickness of 5 mm by removing 2.5 mm of material from both flat sides and for providing a fresh surface just before bonding.

250 g/m² of mixed adhesive (emulsion to hardener ratio of 5:1) were applied homogenously on the flat side of one panel with a spatula, and a second panel was placed immediately on top. For all eight assemblies, the closed waiting time was 15 min, and the press time was 135 min with an applied 1 N/mm² of pressure. Noteworthy, the bonding process was performed in a climate room at 20°C and 65% RH. After pressing, the eight bonded assemblies were stored for 7 days in the same climate and each bonded assembly was cut into 12 specimens for shear test experiments. The resulting 96 specimens were prepared to a length of 140 mm, a width of 20 mm, a thickness of 10 mm, an overlap of 10 mm, and further processed according to the standard DIN EN 302-1:2013. Finally, the specimens were divided into two groups to be treated by (1) A1 Treatment at 20°C and 65% RH (testing in the dry state), and (2) A4 Treatment, which consists of testing the specimens in the wet state after 6 h in boiling water at 100°C followed by 2 h resting in cold water at 20°C. The shear tests were conducted with a universal test machine (112.50kN.L, TesT GmbH) at 20°C and 65% RH, and the wood failure percentage (WFP) was assessed visually.

3 | RESULTS AND DISCUSSION

3.1 | FTIR and NMR analyses of wood extracts and EPI constituents

FTIR experiments were performed on the extracts to identify the chemistry of the compounds present for each wood species and differentiate them. The averaged FTIR

spectra ($n = 3$) of the water extracts are shown in (Figure 1). For revealing differences between the extracts in detail, a principal component analysis (PCA) was applied on the FTIR spectra. The FTIR spectra of the chestnut and oak extracts showed tiny differences between each other (Figure 1a) and based on the PCA results, they were separated from the other extracts by PC1, which explained a high variability of 73% (Figure 1b). The first loading separating the chestnut and oak extracts from others indicated the bands at 1730 cm^{-1} (C=O str. of AcO or COOH), 1317 cm^{-1} (CH_2 def. of cellulose), 1200 cm^{-1} (CH and OH def. of xyloglucan), and 1030 cm^{-1} (C—O str. of cellulose, C—O—C str. of AcO, and C—H plus C—O def. of lignin) (Figure 1b).¹⁷ The strong band at 1730 cm^{-1} in the spectra of chestnut and oak extracts is even visually remarkable (Figure 1a). Therefore, the chemical composition of the chestnut and oak extracts is different from the others due to the higher amount of acetyl (AcO) and/or carboxylic acid (COOH) groups present in the main compounds. This is in line with the higher acidity of the chestnut (pH = 3.8) and oak (pH = 4.2) extracts among the other wood species (pH = 4.6–5.8). Noteworthy, gallic acid—the major component—, sugars and ellagic acid were the identified components of the chestnut water extract.^{9,18}

Liquid ^{13}C NMR and DEPT experiments were conducted on both the extracts and EPI components in order to identify the chemical groups and further help the solid-state NMR evaluation on the cured samples. The analysis of the chestnut extract indicates the presence of gallic acid, together with different monosaccharides and inositol (Figure S3).

3.2 | Analysis of the EPI-adhesive curing

3.2.1 | In situ rheology-FTIR analysis of the EPI-adhesive

Before starting with the systematic investigations, the rheological characteristics of EPI-Ref were studied by strain sweep tests. Under small strain deformation values, the EPI-adhesive showed a mainly elastic character as the storage modulus (G') was already higher than the loss modulus (G'') even at the beginning of the measurements (Figure S4a), and at high strain deformation values, it indicates the shear-thinning nature of this EPI-adhesive coming from the EPI-emulsion component (Figure S4b). For the following systematic tests, to avoid the influence of high deformations and deformation rates on the adhesive curing process, EPI-Ref and EPI-adhesive with extractives were analyzed at the linear viscoelastic region (at 0.1% strain). However, this restricts the evaluation only to the comparison of the flow curves without any determination of a gel point (time point at $G' = G''$) unlike the other structural wood adhesives (e.g., MUF, 1C-PUR, epoxy).^{9,19}

The comparison of the G' curves of the EPI-Ref and EPI-extract mixtures (Table 1) is shown in Figure 2. The technical variabilities within each group were minor (for some examples, see Figure S5). The addition of the chestnut and oak extracts resulted in drastic changes in the G' curves of the EPI-adhesive right from the beginning of the measurements. In particular, the chestnut extract led to a drastic increase in G' (Pa), as G' of EPI-Ref and EPI-Ch were found to be 1014 and 4754 Pa, respectively, at

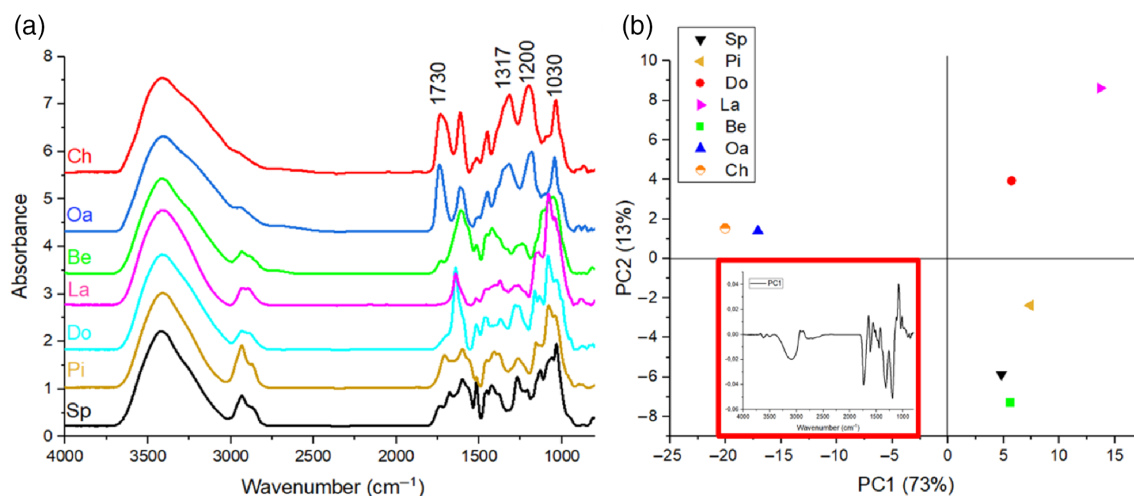


FIGURE 1 (a) Fourier-transform infrared (FTIR) spectra of the water extracts from the studied wood species: Spruce (Sp), pine (Pi), Douglas fir (Do), larch (La), beech (Be), oak (Oa), chestnut (Ch), (b) principal component analysis (PCA) score plots of the FTIR spectra. The inset corresponds to the PC1 loading [Color figure can be viewed at [wileyonlinelibrary.com](https://onlinelibrary.wiley.com)]

$t = 0$ min. At the end of the measurement, $t = 180$ min, G' of EPI-Ch (452 kPa) was still significantly higher than that from EPI-Ref (97 kPa). Comparing the slopes of the curves, both the EPI-Ch and EPI-Oa samples cured faster than the others. Furthermore, the nonlinear development of the curves in both EPI-Ch and EPI-Oa samples indicated different reaction kinetics compared to EPI-Ref and the rest of EPI-extract mixtures (Sp, Pi, Do, La and Be) in which their G' -curves increased almost linearly by time. The differences in the reaction kinetics can be seen from dG'/dt versus measurement time curves as well (Figure S6).

During the EPI-adhesive curing process, the in situ FTIR spectral changes were evaluated for the reference and also the samples showing different rheological properties compared to their reference (Figure 3). Simultaneous reactions took place between the isocyanate (NCO, hardener) and the hydroxyl groups (OH) from the polyol and water molecules from the emulsion component. Moreover, during this curing process, the fast reaction between the isocyanate moiety and a water molecule resulted in carbamic acid formation (NHCOOH), which is unstable and released a CO_2 gas molecule and the corresponding amine formation (NH_2). Therefore, some foaming appeared during the adhesive curing process, which led to changes in the adhesive thickness during the ATR measurements. For that reason, and for a precise evaluation of the spectra, a normalization treatment was required. Due to the presence of calcium carbonate (CaCO_3), which is a common additive in EPI-adhesive formulations, the corresponding sharp peak at 873 cm^{-1} was taken as a reference (Figure S1).²⁰

Finally, the newly formed amine groups and the hydroxyl groups of polyols could react with the isocyanate moieties producing the corresponding urea (NHCONH) and urethane motifs (NHCOO), respectively. As the mobility of water and polyol is different to a higher extent, a higher ratio

of urea to urethane linkage is usually expected in the final cured adhesive composition. By the progress of all these reactions, the chain length of all products increases (polymerization), until achieving a macromolecule by crosslinking.

Although these simultaneous and competitive reactions occur very fast and make the spectral interpretation challenging, some of the curing reactions can be still followed by FTIR spectra. The main characteristic spectral regions for analyzing the curing of the isocyanate-based adhesives can be classified into four groups: (i) $3100\text{--}3500\text{ cm}^{-1}$ (N—H str.),^{21,22} (ii) $2300\text{--}2200\text{ cm}^{-1}$ (NCO str.), (iii) $1700\text{--}1750\text{ cm}^{-1}$ (CO str., urethane and acetyl), and (iv) $1630\text{--}1660\text{ cm}^{-1}$ (amide I urea str., plus —OH str.)^{23–25} (Figure 3). The assignments of these bands and their relative absorbance changes in the samples are given in detail in Table S1. Noteworthy, the broad spectral region in $3100\text{--}3500\text{ cm}^{-1}$ partly overlaps with the —OH stretching (Figure 3a) corresponding to the hydroxyl groups from polyols and water, and the intensity of this peak should decrease upon reacting with the isocyanates groups. Therefore, a direct correlation of the absorbance of this band to the reaction products is not possible because water could also evaporate.

Differences were also found in the spectral region of $1600\text{--}1750\text{ cm}^{-1}$, which mainly assigns for the carbonyl (CO) stretching (Figure 3c). Of note, the absorbance of this band is usually expected to increase by the urethane formation as a result of curing reactions, however, the corresponding changes most likely remain under the influence of the overlapping effects of the components in this current system (Figure S1). In addition, it is known that when urethane is bonded by H-bonds, the band at 1730 cm^{-1} shifts to lower wavenumbers ($\sim 1720\text{ cm}^{-1}$), thus, the absorbance of this band might have been influenced by this fact as well.²⁶ Next to this peak, a

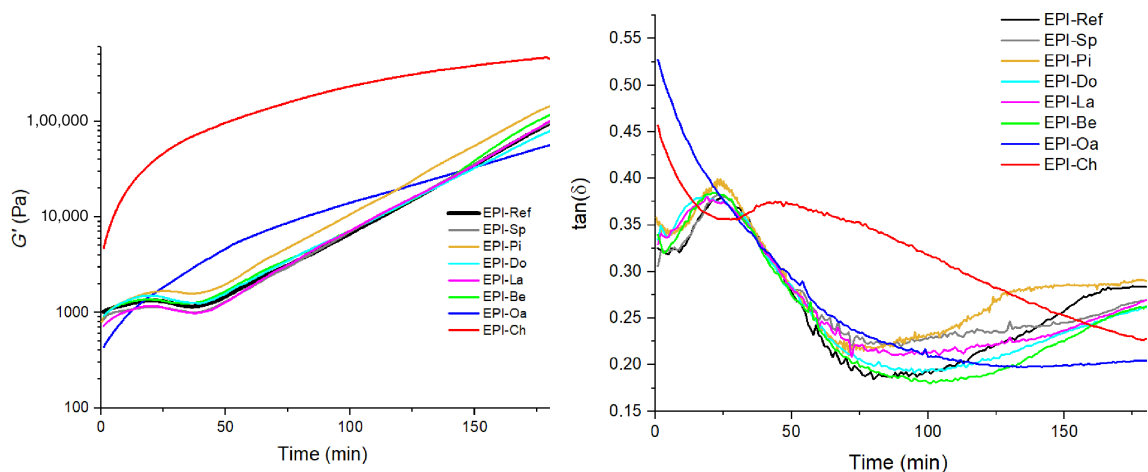


FIGURE 2 The storage modulus (G') and $\tan \delta$ curves of emulsion polymer isocyanate (EPI)-ref (black) and EPI-extract mixtures ($n = 3\text{--}6$, see Table 1) [Color figure can be viewed at wileyonlinelibrary.com]

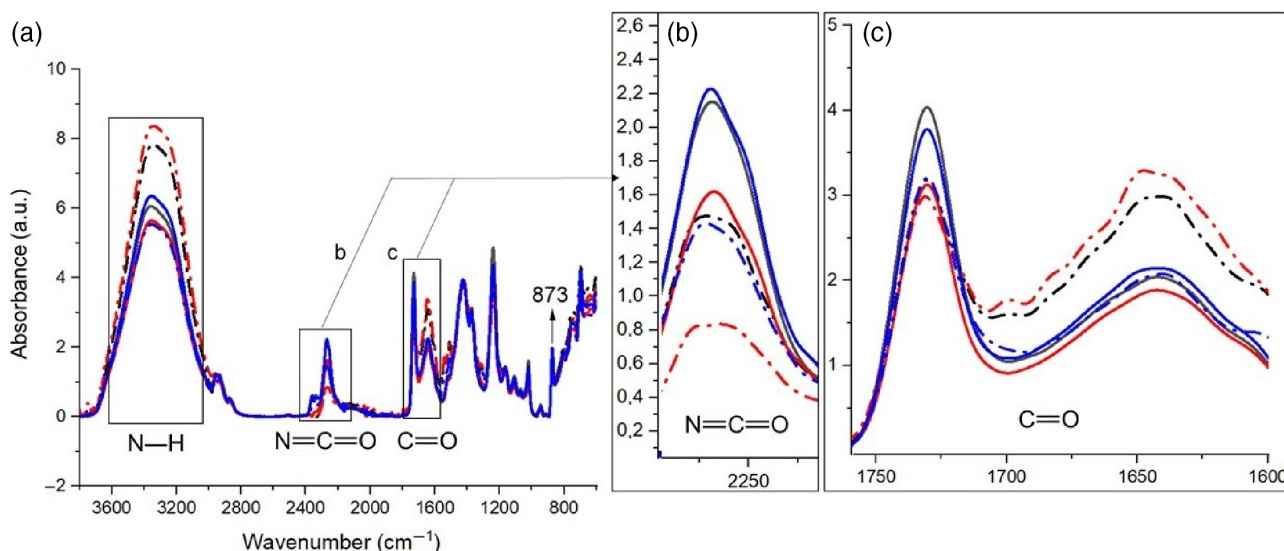


FIGURE 3 Fourier-transform infrared (FTIR) spectra of emulsion polymer isocyanate (EPI)-Ref (black), EPI-Ch (red), and EPI-Oa (blue) at the beginning of the measurements ($t = 0$ min, solid lines) and at the end of the measurements ($t = 180$ min, dashed-dotted lines) in the spectral region of (a) $3700\text{--}3100\text{ cm}^{-1}$ (N—H str. Overlapped with O—H str.), b) $2300\text{--}2200\text{ cm}^{-1}$ (NCO str.), and c) $1750\text{--}1700\text{ cm}^{-1}$ (C=O str. Urethane and acetyl), $1630\text{--}1660\text{ cm}^{-1}$ (amide I urea str., plus —OH str.). All spectra were normalized to the peak at 873 cm^{-1} assigned to the presence of CaCO_3 [Color figure can be viewed at wileyonlinelibrary.com]

shoulder appeared in $1720\text{--}1690\text{ cm}^{-1}$, only in EPI-Ch and EPI-Ref. This shoulder is most likely due to the carbonyl stretching of H-bonded urethane moieties as mentioned above.²³ Of note, the presence of carbonyl groups from extracts and also from the polymers in the water-based EPI-adhesive component – for example, poly(ethylene-vinyl acetate) overlaps with the carbonyl stretching of the urethane in this region $1700\text{--}1750\text{ cm}^{-1}$. All of these make the analysis of the exact chemical reactions highly challenging.

PCA was applied to follow the spectral evolution as a function of the curing time. The main observable chemical changes occurred after 80 min for the EPI-Ref sample (Figure S7a) as PC1, which explains 89% of the variability, divided the spectra into two groups after 80 min. For EPI-Ch and EPI-Oa, the chemical changes occurred much earlier, that is, after 30 and 40 min, respectively (Figure S7b,c). This shows the alterations in the curing kinetics of the EPI-adhesive when chestnut and oak extracts are added, which is in line with the rheology results—that is, acceleration of the network formation as can be seen from G' flow curves.

Furthermore, the loadings, which are responsible for the separation of the groups due to the curing reactions, were compared as well. The loading of the EPI-Ch sample followed a very similar trend to the loading PC1 of the EPI-Ref sample (Figure S8), and mainly indicated the changes based on the peaks at 3353 cm^{-1} (NH str.), 2272 cm^{-1} (NCO str.), and 1650 cm^{-1} (amide I urea str.).^{23,24,27–29} Considering similar loadings, it can be concluded that similar compounds react and form similar

products for both the EPI-Ref and EPI-Ch samples, but with different reaction kinetics.

When comparing the loading PC1 of the EPI-Oa sample with the EPI-Ref and EPI-Ch, some differences can be observed (Figure S8). First of all, the loading of EPI-Oa showed an opposite direction for the peak at 3353 cm^{-1} (NH str.) and 1650 cm^{-1} (amide I urea str.). In EPI-Oa, the absorbance at these band positions decreased by time, unlike the other samples. Furthermore, on the contrary to the loadings of EPI-Ref and EPI-Ch, almost all bands: for example, 1540 cm^{-1} (N—H bend., CN str.), 1509 cm^{-1} (N—H bend., C=C str.), 1447 cm^{-1} (—CH, —CH₂), 1307 cm^{-1} (CN str., NH bend. and CH in benzene ring), 1241 cm^{-1} (C—N str., C—O str. of urethane) and 1209 cm^{-1} (amide III, C—O str.),^{30–32} contributed to the loading 1 of EPI-Oa. These results indicate different curing reactions in EPI-Oa compared to EPI-Ref and EPI-Ch. However, all of these aforementioned bands are unspecific which complicates the interpretation of the curing reactions. Of note, how both the oak and chestnut extracts influence the EPI-curing will be investigated further in the following chapter.

3.2.2 | Understanding the specific interactions between the chestnut and oak extractives and EPI-adhesive

The chestnut and oak extracts are known to be rich in tannin-based compounds, which can be classified as

hydrolyzable and condensed tannins. Hydrolyzable tannins consist of a central core of glucose together with gallic acid derivatives.^{33,34} The previous GC/MS analysis of the water chestnut extract revealed the presence of gallic acid as a major compound together with some sugars and ellagic acid in the composition.¹⁸ Moreover, based on the FTIR analysis, the chemistry of the chestnut and the oak extracts were similar to each other to a large extent (Figure 1).

However, previously, PC loadings (FTIR analysis) indicated different curing reactions between EPI-Ch and EPI-Oa (Figure S8). Therefore, it was necessary to further investigate whether the differences in the adhesive curing reactions between the EPI-Ch and EPI-Oa samples were only due to slight compositional differences between the two extractives or due to the different amounts of the extractives mixed to the EPI adhesive (0.9% for EPI-Ch and 0.17% for EPI-Oa, Table 1). For clarifying this point, additional rheology measurements were performed with an exchanged amount of the extracts (0.90% for EPI-Oa and 0.17% for EPI-Ch) mixed to the adhesive.

When the same amounts of the extracts were added to the EPI-adhesive, similar rheological properties were found between the EPI-Ch and EPI-Oa samples (Figure 4). Based on PCA results from the FTIR spectra, also similar chemical reactions were found between both samples (Figure S9). Therefore, it can be concluded that both the chestnut and oak extracts similarly influenced the EPI-adhesive curing process. However, the amounts of added extracts to EPI-adhesive determined the speed of the reaction and, therefore, the crosslinking process of the adhesive at $t = 180$ min (not fully cured state). For the comparison of the final crosslinking of the adhesive at the fully cured state, the readers are referred to Section 3.3.

Some additional experiments were performed by adding some carboxylic acid or phenolic compounds to the EPI-adhesive for revealing more details on the effects during the curing process. The addition of gallic acid—as the main component of the chestnut extract—also resulted in a similar acceleration (catalysis) on the curing process as observed for the EPI-Ch and EPI-Oa sample (Figure S10) and this effect became more pronounced with increasing the amount of gallic acid to the EPI-adhesive. Similarly, measurements with benzoic acid confirmed that aromatic carboxylic acids speed up the curing process of the EPI-adhesive (Figure S11), while phenolic compounds—for example, phloroglucinol and hydroquinone—and hydroxycinnamic acids—for example, coumaric acid, caffeic acid, and ellagic acid—speed up the curing process moderately. However, aliphatic acids—for example, succinic acid, malonic acid, and maleic acid—and sugar alcohol—for example, xylitol—did not change the curing kinetics significantly (for the comparison of the pKa values of the compounds, see Table S2). Taken all results together, it is clear that the acidity of groups bound at an aromatic skeletal structure has a catalytic effect in the EPI-adhesive curing process. This might be due to structural similarities with the polyisocyanate hardener allowing for a good mixing between those aromatic compounds and the aromatic crosslinker by means of π - π interactions.

Noteworthy, despite to pronounced influences of the aromatic carboxylic acids and phenolic compounds on the EPI-adhesive curing process, no clear separation could be found in the final FTIR spectra most probably due to the small amounts of such chemicals in the final mixture.

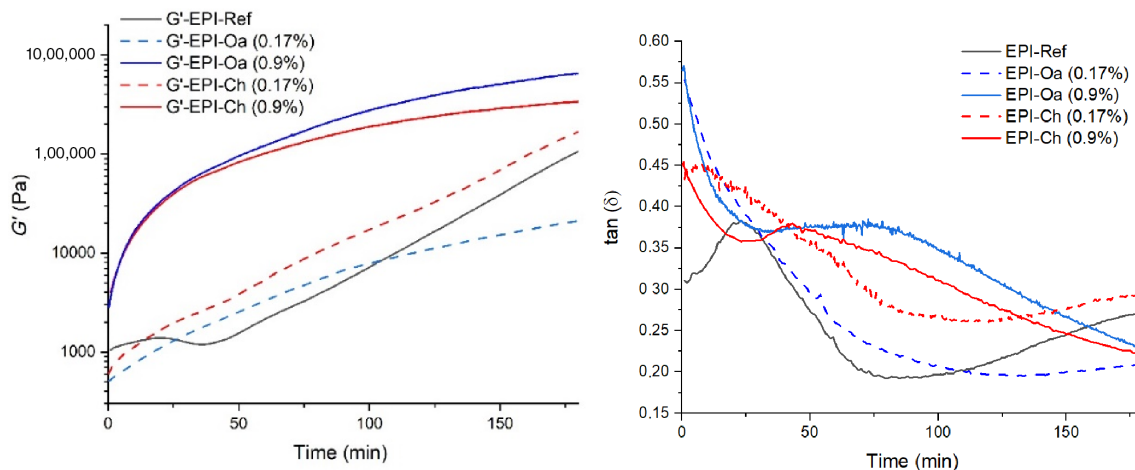


FIGURE 4 Storage shear modulus G' (left) and $\tan \delta$ curves as a function of time (right) for the emulsion polymer isocyanate (EPI)-Ch and EPI-Oa samples with 0.90% and 0.17% of extracts compared to references [Color figure can be viewed at wileyonlinelibrary.com]

3.2.3 | Evolved gas analysis

According to in situ rheology FTIR analysis results, the most significant changes between the EPI-Ref and the combination of EPI-adhesive with acidic extracts have been observed in the first couple of hours. However, the exact chemical reactions could not be identified by FTIR spectroscopy due to the methodological limitations, for example, overlapped bands. In this respect, EGA and pyrolysis measurements can be used as complementary techniques to reveal the chemical curing reactions further.

The EGA is an analytical method to differentiate qualitatively the thermal behavior of substances due to their evaporation and therefore their mass and constitution. In the current study, by analyzing the evolved gases from the samples, differences in the polymerization and crosslinking degree of the adhesive were estimated. For a reasonable comparison of rheology and EGA results, EGA measurements were performed immediately after the Rheonaut measurements—after 3 h—on some selected samples, that is, EPI-Ref and EPI-Ch (0.90%) at the not fully cured state. Considering the sample preparation and measurement time (device preparation, heating time, etc.), the EPI-adhesive was analyzed at 3.5–4 h of the cured state. In line with the rheology results, some differences were also found in the EGA thermal profiles and showed a different crosslinking degree of the adhesive with the presence of the chestnut extract at this time (Figure 5). In the EPI-Ch sample, a new peak could be detected at 200°C, whereas, in the EPI-Ref sample, a clear gas evolution (shoulder) was only observed starting from 250°C on. The thermal profiles of the samples did not differ significantly after 350°C. For both samples, the maximum gas abundance was observed around 400°C. In addition, some gases were evolved around 620°C.

3.2.4 | Double shot analysis with GC/MS

Based on EGA results, a new band appeared at 200°C in EPI-Ch (Figure 5). Using two-stage DSA measurements, the chemical composition of the evolved volatiles at 200°C and also its' neighbor band at 310°C was analyzed through: (i) thermal desorption (TD) at 200°C, and (ii) Pyrolysis (Py) at 310°C.

The chromatograms from the TD at 200°C are shown in Figure 6a. The total abundance of the volatile components did not differ significantly between both the EPI-Ref and EPI-Ch samples, however, some differences were observed in the proportions of the identified compounds. Methylenedianiline (MDA, at 21.7 and 22.4 min) was the major compound in both samples. However, in the EPI-

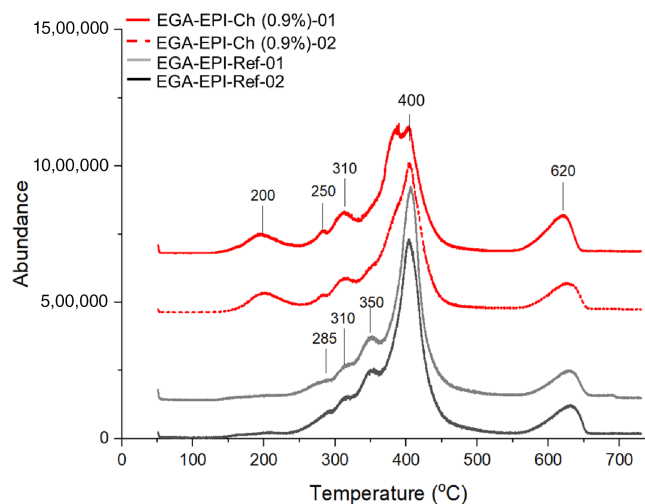


FIGURE 5 Evolved gas analysis (EGA) thermal profiles of the emulsion polymer isocyanate (EPI)-Ref and EPI-Ch (0.9%) sample (the graphs were plotted stacked in the Y-axis for better visualization) [Color figure can be viewed at wileyonlinelibrary.com]

Ch sample, a higher amount of isocyanatobenzylaniline (at 21.2 min)³⁵ and methylene diphenyl diisocyanate (MDI, at 19.5 min and 20.2 min) were present besides the MDA peak. The overall relative amount of MDA concerning the other compounds (isocyanatobenzylaniline and MDI) was 43% higher (based on peak heights) in the EPI-Ref compared to the EPI-Ch sample.

The chromatograms obtained by pyrolysis at 310°C showed a clear difference in the abundance of the total volatile components, which was in total 144% higher (based on peak heights) in the EPI-Ch sample compared to the EPI-Ref sample (Figure 6b). The MS spectra of EPI-Ch showed basically the presence of MDI molecules coming from the fission of urethane moieties, while MDA was still detectable for the EPI-Ref sample. Of note, while MDA represents a byproduct from the hydrolysis of MDI, the detected MDI indicates either the presence of unreacted hardener (DSA-TD) or from the decomposition of urethane moieties (DSA-Py) as similar results were observed by the pyrolysis experiments of the pure hardener (Figure S12).

This difference in the MDA/MDI ratio from DSA-TD experiment at 200°C can be explained due to the fast curing of the EPI adhesive in the presence of the acidic chestnut extracts, while the pure adhesive cures slower allowing for a higher degree of hydrolysis of the isocyanate molecules (MDI) into amines (MDA and isocyanatobenzylaniline). This result was also confirmed by the DSA-Py experiments at 310°C that show an increase of the amount of MDI due to the decomposition of the urethane linkages formed during the curing

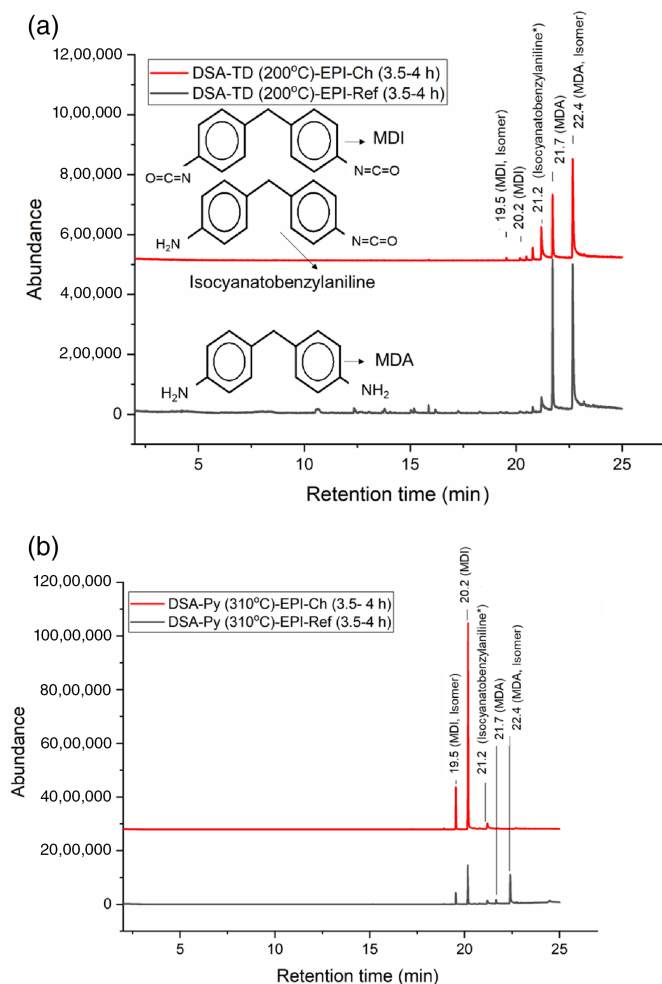


FIGURE 6 Double shot analysis (DSA) chromatograms of the emulsion polymer isocyanate (EPI)-Ref, EPI-Oa, and EPI-Ch samples (3 h, directly after Rheonaut measurements). (a) Thermal desorption at 200°C and (b) pyrolysis at 310°C. The peak at 21.2 min could not be found in the database, however, molecular mass calculations from mass spectra are in line with isocyanatobenzylaniline ($m/z = 224$ Da), similar MS spectra were shown also in reference 35. The graphs were plotted stacked in the Y-axis for better visualization [Color figure can be viewed at wileyonlinelibrary.com]

process that is higher for the EPI-Ch sample than for the EPI-Ref sample due to more advanced reaction progress for the former.

It seems that at the analysis time interval (3.5–4 h), the presence of the chestnut extract impedes the reaction of the isocyanates to form the final reaction products as in both thermal desorption and pyrolysis experiments, as a higher MDI/MDA ratio was found in EPI-Ch, whereas, in between 0–3 h, the isocyanate consumption (based on the absorbance of the FTIR band at 2275 cm^{-1}) was higher in EPI-Ch compared to EPI-Ref. Taken these results together, it can be concluded that the addition of the chestnut extract led to a drastic increase in the

reaction speed and less amount of free anilines from the hydrolysis of isocyanates at this analysis time interval. This can be because the mobility of the molecules was most likely restricted after 3 h due to a high viscosity increase in the media, which in turn slows down the final steps of the curing process. This is in line with the rheology results (i.e., G' curves and dG'/dt values) when measured for a longer period of 6 h (Figure S13).

3.3 | Analysis of the fully cured EPI-adhesive

3.3.1 | Longer time rheology measurements

Previous investigations revealed the significant influence of the chestnut and oak extracts on the EPI-adhesive curing process. However, these investigations analyzed the properties of the partially cured adhesives. For this reason, to conclude on the final crosslinking of the samples (through G' -modulus values), it was necessary to perform longer time rheological measurements until the adhesive was fully cured. The comparison of the G' values after 36 h is shown in Figure 7, (for the dG'/dt values as a function time, see Figure S14. Apparently, despite significant interactions between the acidic extracts and EPI-adhesive during the first couple of hours, the samples reached a similar plateau of G' values after ~ 24 h. Therefore, the extracts seemed to be more influential on the curing kinetics rather than the final adhesive strength and crosslinking of the fully cured resin.

3.3.2 | Solid-state ^{13}C nuclear magnetic resonance

In order to reveal the chemical and supramolecular structure of the fully cured EPI-adhesive in more detail, solid-state ^{13}C NMR (ssNMR) analyses were performed on 2 months old EPI-Ref, EPI-Ch, and EPI-Oa cured samples (Figure 8). ssNMR is a valuable technique that allows for the qualitative and quantitative chemical analysis of insoluble or nonvolatile materials, for example, crosslinked polymers, which cannot be analyzed or quantified by techniques such as MS, UV-Vis, or FTIR. Both EPI-Ch and EPI-Oa samples were compared with the EPI-Ref to detect the presence of the corresponding extractives. At first sight, the NMR spectra of all EPI-adhesive samples look the same.

The ssNMR spectrum of the EPI-Ref sample (Figure 8, Figure S15) showed the presence of the polymer (PVA-PVAc) from the EPI-emulsion before and after crosslinking. The acetyl groups were identified from the

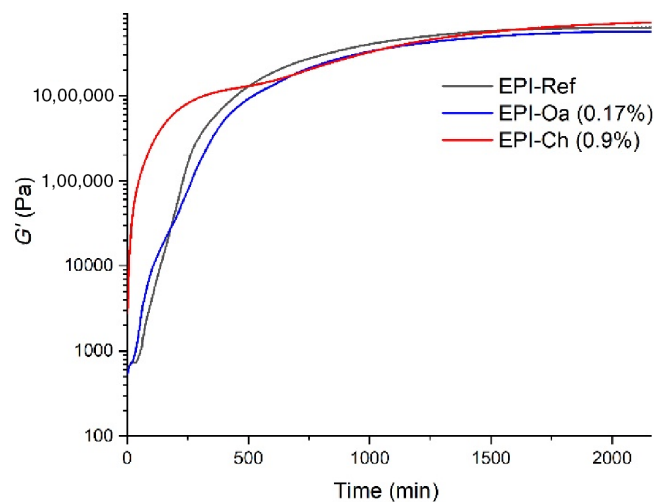


FIGURE 7 The comparison of the storage shear modulus G' curves after 36 h for the emulsion polymer isocyanate (EPI)-Ref, EPI-Ch, and EPI-Oa samples [Color figure can be viewed at wileyonlinelibrary.com]

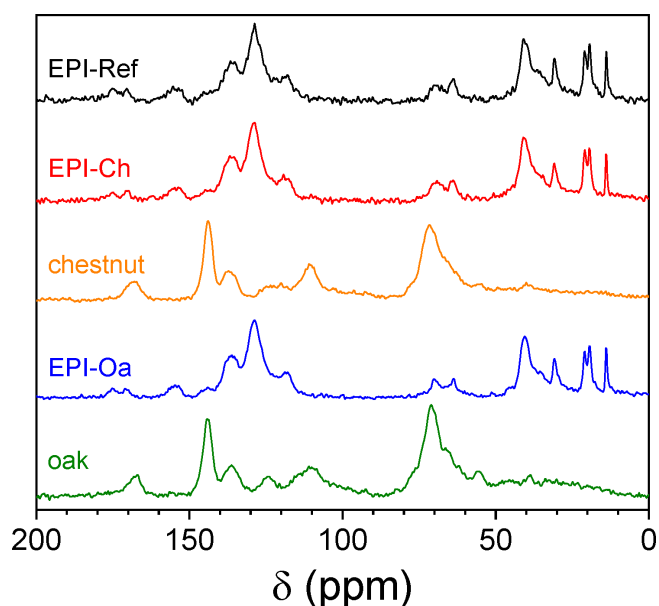


FIGURE 8 Solid-state ^{13}C NMR spectra for the emulsion polymer isocyanate (EPI)-Ref (black), EPI-Ch (0.93%, red), EPI-Oa (0.17%, blue) samples, and the chestnut (orange) and oak (green) extracts [Color figure can be viewed at wileyonlinelibrary.com]

peaks at 170 and 175 ppm, and at 19 and 21 ppm, which corresponded to the carbonyl (CO) and methyl (CH_3) moieties, respectively, in the acetyl group ($\text{Ac} = \text{CH}_3\text{CO}$). The broad peaks centered at 69 and 41 ppm were assigned to the tertiary ($\text{CH}-\text{O}$) and secondary (CH_2) carbons from the polymer backbone, respectively. At the same time, the peaks corresponding to the carbonyl groups from both urea and urethane moieties were

detected at 156 ppm, the aromatic carbons from the reacted EPI-hardener at 118, 130, 136, and 145 ppm, and the methylene group (CH_2) at 42 ppm.

The ssNMR spectrum of the chestnut extract (Figure 8, Figure S16) clearly indicates the presence of gallic acid moieties from the broad peak centered at 168 ppm corresponding to the carboxylic acid group (COOH), and the four aromatic carbons at 110, 122, 137, and 144 ppm. A strong broad signal at 72 ppm from the tertiary carbons ($\text{CH}-\text{O}$), and the broad signals at 92–102 and at 61–71 ppm corresponding to the anomeric ($\text{O}-\text{CH}-\text{OH}$) and the secondary (CH_2-OH) carbons, respectively, from the different α - and β -monosaccharides, for example, glucose, arabinose, and xylose in both the pyranose or furanose forms, were detected together with the tertiary carbons ($\text{CH}-\text{OH}$) from inositol at 72 ppm.

A deconvolution process was conducted in both EPI-Ch and EPI-Oa samples to detect the differences detectable by solid-state ^{13}C NMR and to calculate the percentage of extract from the spectra by adjusting the percentage contribution of both the EPI-Ref and the corresponding extract spectra. The resulting fitting curve was the optimal through the minimum sum of squared deviations. The results show a quite good matching with the initial composition of both the EPI-Ch (0.93%) and EPI-Oa (0.17%) samples from which 0.98% and 0.35% of extracts were detected, respectively (Figure S17).

Obviously, despite significant alterations in the early curing reactions with the addition of the extracts, after all curing reactions are completed; the chemical composition of the samples did not differ significantly from each other as shown from the results obtained by ssNMR analysis. This is in line with the longer time rheology measurements (after 36 h), as all samples reached a similar plateau in the G' modulus although their starting modulus was significantly different at the beginning of the measurements.

3.3.3 | Mechanical analysis

Extraction results of the wood boards selected for the mechanical analysis

The extraction results of the chestnut wood boards are given in Figure S2b. The extracted amount achieved from each glass container was comparable with each other. On average, 1.97% of the extract was obtained, which was comparable also with the previous study.⁹

Mechanical lap shear test results

The mechanical test results showed a minor influence of the extraction on the shear strength values. The average

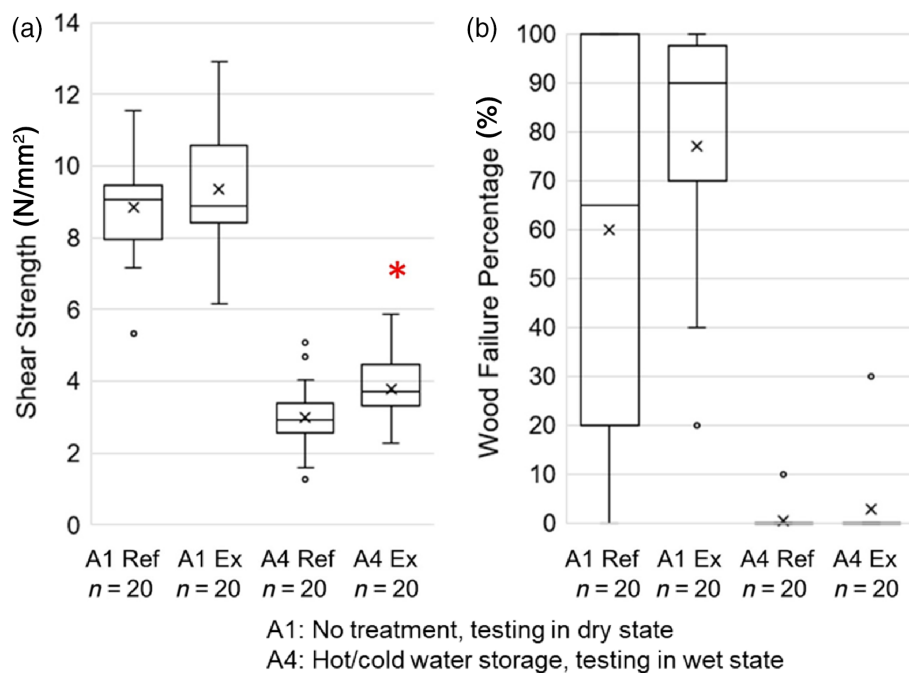


FIGURE 9 Mechanical test results on emulsion polymer isocyanate (EPI)-glued chestnut wood samples and under different treatments—A1: no treatment, testing in dry state; and A4: hot/cold water storage, testing in wet state (a) shear strength, and (b) wood failure percentage (Ref: non-extracted chestnut wood; Ex: cold water extracted chestnut wood. * indicates statistical difference, *t*-test, α : 0.05) [Color figure can be viewed at wileyonlinelibrary.com]

shear strength in the case of both treatments - A1 and A4 - was slightly higher for the extracted chestnut wood samples compared to the non-extracted, reference sample, and the *t*-test was revealed a statistically significant difference only for A4 treatment results (Figure 9a). The results are in line with a slightly higher WFP of the extracted specimens (Figure 9b).

Although the curing properties of the EPI-adhesive was affected drastically by the chestnut extract at the initial phase of the curing reactions (3–4 h), which speeded up the crosslinking process, no major difference could be found in the G' modulus after 36 h upon reaching the plateau (Figure 7). Despite this, the G' modulus was 15% higher and 10% lower for the EPI-Ch and the EPI-Oa, respectively, with respect to the EPI-Ref sample. In Table S3, the storage shear modulus G' after 36 h of curing, the corresponding segmental molecular weight, and the crosslinking density are shown for the samples EPI-Ref, EPI-Ch, and EPI-Oa after complete curing.

In addition, the solid state-NMR results confirmed the similar chemical structures between the fully cured EPI-Ref and both EPI-Ch and EPI-Oa mixtures. Therefore, the observed minor changes in the bonding strength can be considered in line with the previous results. If it is assumed that the chestnut extract has no big impact on the mechanical properties of the fully cured adhesive, the minor changes in the bonding strength of the shear specimens could be also due to a different penetration or wetting behavior of the adhesive as a result of the adhesive interactions with the extracts (i.e., higher starting

viscosity in EPI-Ch compared to EPI-Ref, see Figure 7). This needs to be confirmed by additional future investigations.

4 | CONCLUSION

In this study, the interactions of an EPI adhesive with water extracts from several wood species were systematically investigated. The results showed that tannin-rich, chestnut, and oak acidic extracts have significant influences on the EPI adhesive curing process. In particular, the addition of these extracts to EPI adhesive catalyzed the curing reactions, which in turn led to a drastic increase in the adhesive viscosity, in particular, in the first couple of reaction hours. After that, due to such a high increase in viscosity, the rate of the curing reactions slowed down significantly. The level of all these alterations was highly dependent on the extract amount added to the EPI adhesive. However, despite significant influences of the chestnut and oak extract compositions on the curing kinetics, the final chemical structure of the fully cured adhesive was not significantly different between with or without the presence of such extracts, as revealed by solid-state NMR. Similarly, when testing the mechanical properties of the fully cured adhesive using rheological measurements until 36 h and also tensile shear tests, the influence of the extracts was minor.

Nevertheless, this study shows that special attention is required when bonding wood species with high acidity and high extract content. Such a fast increase in the

adhesive viscosity is due to the advance of the chemical progress catalyzed by this kind of acidic extracts, which might create some problems not only in the wood bonding process (e.g., preparation, application time) but also in the bonding quality (e.g., less adhesive penetration, partial curing, etc.).

Finally, the study shows the potential of this research field for ensuring reliable wood-based assemblies based on hardwood species with high natural durability, as oak and chestnut. Using such specific analyses, the interactions between the chemical constituents of wood and adhesives can be revealed, which in turn, allows for the specific adjustments on the adhesive formulations or the wood surface (e.g., application of a primer for the adjustment of surface pH) for achieving a high quality of the wood-adhesive bonds.

ACKNOWLEDGMENTS

This research work is funded by the German Federal Ministry for Economic Affairs and Energy (Bundesministerium für Wirtschaft und Energie (BMWi) and managed by the German Federation of Industrial Research Associations (AiF) and the Int. Association for Technical Issues related to Wood (iVTH), (Project number IGF 19314 N). The authors thank for financial support. The authors also thank Dynea for providing the adhesive materials. Open Access funding enabled and organized by Projekt DEAL.

CONFLICT OF INTEREST

The authors declare no potential conflict of interest.

AUTHOR CONTRIBUTIONS

Merve Özparpucu designed and performed the rheology, spectroscopy and thermal analysis experiments, evaluated the results, and wrote the manuscript. Antoni Sánchez-Ferrer performed the liquid NMR experiments, evaluated and analyzed the results of both liquid and solid-state NMR, revised and co-wrote the manuscript. Mathias Schuh and Bianca Wilhelm performed lap tensile shear tests and evaluated the results. Riddhiman Sarkar and Bernd Reif performed the solid-state NMR experiments. Elisabeth Windeisen-Holzhauser and Klaus Richter designed and supervised the study, revised the manuscript.


DATA AVAILABILITY STATEMENT

Research data are not shared.

ORCID

Merve Özparpucu  <https://orcid.org/0000-0002-0822-6552>

Antoni Sánchez-Ferrer  <https://orcid.org/0000-0002-1041-0324>

Riddhiman Sarkar  <https://orcid.org/0000-0001-9055-7897>

Bernd Reif  <https://orcid.org/0000-0001-7368-7198>

Klaus Richter  <https://orcid.org/0000-0002-6583-0254>

REFERENCES

- [1] J. L. Howard, S. Liang, *United States Forest Products Annual Market Review and Prospects: 2005–2019*, Madison, Wisconsin, USA **2019**.
- [2] P. Blanchet, C. Breton, *For.: Wood Prod. Renew. Mater.* **2020**, *11*(6), 657.
- [3] A. W. Christiansen, *Wood Fiber Sci.* **2007**, *22*, 441.
- [4] M. S. White, G. Ifju, J. A. Johnson, *Wood Fiber Sci.* **2007**, *5*, 353.
- [5] D. C. Maldas, D. P. Kamdem, *For. Prod. J.* **1999**, *49*, 91.
- [6] R. Subramanian, *The Chemistry of Solid Wood*. Advances in Chemistry Series. ACS Publication, Washington, DC **1984**, Ch.7, pp. 291–305. <https://pubs.acs.org/doi/10.1021/ba-1984-0207.ch007>.
- [7] C.-Y. Hse, M.-I. Kuo, *For. Prod. J.* **1988**, *38*(1), 52.
- [8] S.-i. Tohmura, *J. Wood Sci.* **1998**, *44*, 211.
- [9] M. Özparpucu, T. Wolfrum, E. Windeisen-Holzhauser, M. Knorz, K. Richter, *Eur. J. Wood Wood Prod.* **2020**, *78*, 85.
- [10] K. Grøstad, A. Pedersen, *J. Adhes. Sci. Technol.* **2010**, *24*, 1357.
- [11] J. Guo, H. Hu, K. Zhang, Y. He, X. Guo, *Polymer* **2018**, *10*, 652.
- [12] X. Wang, O. Hagman, B. Sundqvist, S. Ormarsson, H. Wan, P. Niemz, *Eur. J. Wood Wood Prod.* **2015**, *73*, 225.
- [13] L. Qiao, A. J. Easteal, C. J. Bolt, P. K. Coveny, R. A. Franich, *Pigm. Resin Technol.* **2000**, *29*, 4.
- [14] P. Solt, J. Konnerth, W. Gindl-Altmutter, W. Kantner, J. Moser, R. Mitter, H. W. van Herwijnen, *Int. J. Adhes. Adhes.* **2019**, *94*, 99.
- [15] K. Grøstad, R. Bredesen, *Materials and Joints in Timber Structures*. Springer, Dordrecht, The Netherlands **2014**, pp. 355–364. https://link.springer.com/chapter/10.1007%2F978-94-007-7811-5_32.
- [16] F. Meyer, M. Feustel, J. Plog, Proceedings, 70th Annual Technical Conference of the Society of Plastics Engineers, ANTEC, Orlando, Florida, USA **2012**, *1*, 48–50.
- [17] N. Gierlinger, L. Goswami, M. Schmidt, I. Burgert, C. Coutand, T. Rogge, M. Schwanninger, *Biomacromolecules* **2008**, *9*, 2194.
- [18] T. Wolfrum, M. Knorz, E. Windeisen-Holzhauser, K. Richter, *iGF Project Nr. 19314 N* **2017**, Interim report.
- [19] G. Stapf, N. Zisi, S. Aicher, *Pro Ligno* **2013**, *9*.
- [20] N. Hori, K. Asai, A. Takemura, *J. Wood Sci.* **2008**, *54*, 294.
- [21] A. Sánchez-Ferrer, D. Rogez, P. Martinoty, *Macromol. Chem. Phys.* **2010**, *211*, 1712.
- [22] A. Sánchez-Ferrer, D. Rogez, P. Martinoty, *RSC Adv.* **2015**, *5*, 6758.
- [23] A. L. Daniel-da-Silva, J. C. M. Bordado, J. M. Martín-Martínez, *J. Appl. Polym. Sci.* **2008**, *107*, 700.
- [24] M. Szycher, *Szycher's Handbook of Polyurethanes*. CRC Press, Boca Raton, FL, USA **2012**, p. 37.
- [25] R. J. Marathe, A. B. Chaudhari, R. K. Hedao, D. Sohn, V. R. Chaudhari, V. V. Gite, *RSC Adv.* **2015**, *5*, 15539.
- [26] D. Ren, C. E. Frazier, *Int. J. Adhes. Adhes.* **2013**, *45*, 118.
- [27] H. Hao, J. Shao, Y. Deng, S. He, F. Luo, Y. Wu, J. Li, H. Tan, J. Li, Q. Fu, *Biomater. Sci.* **2016**, *4*, 1682.
- [28] M. Sultan, K. M. Zia, H. N. Bhatti, T. Jamil, R. Hussain, M. Zuber, *Carbohydr. Polym.* **2012**, *87*, 397.
- [29] A. Marcos-Fernandez, A. Lozano, L. Gonzalez, A. Rodriguez, *Macromolecules* **1997**, *30*, 3584.

- [30] V. Romanova, V. Begishev, V. Karmanov, A. Kondyurin, M. F. Maitz, *J. Raman Spectrosc.* **2002**, *33*, 769.
- [31] S. J. McCarthy, G. F. Meijs, N. Mitchell, P. A. Gunatillake, G. Heath, A. Brandwood, K. Schindhelm, *Biomaterials* **1997**, *18*, 1387.
- [32] C. Tan, T. Tirri, C.-E. Wilen, *Polymer* **2017**, *9*, 184.
- [33] D. Fengel, G. Wegener, *Wood: Chemistry, Ultrastructure, Reactions*, Walter de Gruyter, Berlin, Germany **1983**. <https://www.degruyter.com/document/doi/10.1515/9783110839654/html?lang=en>.
- [34] G. Wischer, J. Boguhn, H. Steingaß, M. Schollenberger, M. Rodehutsord, *Animal* **2013**, *7*, 1796.
- [35] E. A. Larson, J. Lee, A. Paulson, Y. J. Lee, *J. Am. Soc. Mass Spectrom.* **2019**, *30*, 1046.

SUPPORTING INFORMATION

Additional supporting information may be found in the online version of the article at the publisher's website.

How to cite this article: M. Özparpucu, A. Sánchez-Ferrer, M. Schuh, B. Wilhelm, R. Sarkar, B. Reif, E. Windeisen-Holzhauser, K. Richter, *J. Appl. Polym. Sci.* **2022**, *139*(21), e52189. <https://doi.org/10.1002/app.52189>